



Pithoviruses Are Invaded by Repeats That Contribute to Their Evolution and Divergence from Cedratviruses

Sofia Rigou, Alain Schmitt, Jean-Marie Alempic, Audrey Lartigue, Peter Vendlozki, Chantal Abergel, Jean-Michel Claverie, Matthieu Legendre

► To cite this version:

Sofia Rigou, Alain Schmitt, Jean-Marie Alempic, Audrey Lartigue, Peter Vendlozki, et al.. Pithoviruses Are Invaded by Repeats That Contribute to Their Evolution and Divergence from Cedratviruses. *Molecular Biology and Evolution*, 2023, 10.1093/molbev/msad244 . hal-04299501

HAL Id: hal-04299501


<https://hal.science/hal-04299501>

Submitted on 22 Nov 2023

HAL is a multi-disciplinary open access archive for the deposit and dissemination of scientific research documents, whether they are published or not. The documents may come from teaching and research institutions in France or abroad, or from public or private research centers.

L'archive ouverte pluridisciplinaire **HAL**, est destinée au dépôt et à la diffusion de documents scientifiques de niveau recherche, publiés ou non, émanant des établissements d'enseignement et de recherche français ou étrangers, des laboratoires publics ou privés.

Pithoviruses Are Invaded by Repeats That Contribute to Their Evolution and Divergence from Cedratviruses

Sofia Rigou,¹ Alain Schmitt,¹ Jean-Marie Alempic,¹ Audrey Lartigue,¹ Peter Vendloczki,¹ Chantal Abergel,¹ Jean-Michel Claverie ¹, and Matthieu Legendre ^{1,*}

¹Information Génomique & Structurale, Unité Mixte de Recherche 7256 (Institut de Microbiologie de la Méditerranée, FR3479), IM2B, IOM, Aix-Marseille University, Centre National de la Recherche Scientifique, Marseille 13288 Cedex 9, France

*Corresponding author: E-mail: legendre@igs.cnrs-mrs.fr.

Associate editor: Crystal Hepp

Abstract

Pithoviridae are amoeba-infecting giant viruses possessing the largest viral particles known so far. Since the discovery of *Pithovirus sibericum*, recovered from a 30,000-yr-old permafrost sample, other pithoviruses, and related cedratviruses, were isolated from various terrestrial and aquatic samples. Here, we report the isolation and genome sequencing of 2 *Pithoviridae* from soil samples, in addition to 3 other recent isolates. Using the 12 available genome sequences, we conducted a thorough comparative genomic study of the *Pithoviridae* family to decipher the organization and evolution of their genomes. Our study reveals a nonuniform genome organization in 2 main regions: 1 concentrating core genes and another gene duplications. We also found that *Pithoviridae* genomes are more conservative than other families of giant viruses, with a low and stable proportion (5% to 7%) of genes originating from horizontal transfers. Genome size variation within the family is mainly due to variations in gene duplication rates (from 14% to 28%) and massive invasion by inverted repeats. While these repeated elements are absent from cedratviruses, repeat-rich regions cover as much as a quarter of the pithoviruses genomes. These regions, identified using a dedicated pipeline, are hotspots of mutations, gene capture events, and genomic rearrangements that contribute to their evolution.

Key words: giant viruses, comparative genomics, genome evolution.

Introduction

Pithoviridae are amoeba-infecting giant viruses possessing the largest known viral particles. The prototype of the family, *Pithovirus sibericum*, was recovered almost 10 yr ago from a 30'000-yr-old permafrost sample (Legendre et al. 2014). Following this discovery, 6 additional isolates, all infecting *Acanthamoeba castellanii*, have been sequenced (Andreani et al. 2016; Levasseur et al. 2016; Bertelli et al. 2017; Rodrigues et al. 2018; Jeudy et al. 2020). Their dsDNA circular genomes range from 460 to 686 kb. The *Pithoviridae* are composed of 2 main clades: the pithoviruses and the cedratviruses. Both possess ovoid-shaped virions, capped by a cork-like structure at 1 extremity for the former and at both extremities for the latter.

Pithoviridae have mostly been isolated from permafrost (Legendre et al. 2014; Jeudy et al. 2020; Alempic et al. 2023) and sewage samples (Levasseur et al. 2016; Silva et al. 2018). Metagenomic surveys have also revealed *Pithoviridae*-like sequences in deep-sea sediments (Bäckström et al. 2019), in forest soil samples (Schulz et al. 2018), and their high abundance in permafrost (Rigou et al. 2022). In every case, a phylogeny of the metagenomic viral sequences showed that they branch outside the clade of isolated *Pithoviridae*, suggesting that new viral species are yet to be discovered (Rigou et al. 2022).

Genomic gigantism has been observed several times in the virosphere, among viruses infecting prokaryotes, such as “huge” (Al-Shayeb et al. 2020) and “jumbo” phages (Yuan and Gao 2017), or eukaryotes, as in the *Nucleocytoviricota* phylum to which the *Pithoviridae* family belongs. But its origin remains a mystery as most giant virus genes have no known origin. Furthermore, *Pithoviridae* and their relatives are good models to study viral gigantism as there is a variety of genome (and virion) size among the viral order they belong to: the *Pimascovirales* (Lefkowitz et al. 2018; Koonin et al. 2020). The latter is formed by *Iridoviridae*, *Ascoviridae*, and *Marseilleviridae* on one side and *Pithoviridae*, *Orpheovirus*, and related viruses known from metagenomics such as *Hydriviruses* (Rigou et al. 2022) on the other side. The closest isolated relative to *Pithoviridae* is *Orpheovirus*, with a much larger, 1.6 Mb, genome (Andreani et al. 2018). *Orpheovirus* infects *Vermamoeba vermiformis*, while *Pithoviridae* and *Marseilleviridae* both infect *Acanthamoeba*. Some authors consider *Orpheovirus* to be part of *Pithoviridae* (Aylward et al. 2021), although we chose not to, considering the few genes they share (Andreani et al. 2018; Queiroz et al. 2023). *Hydrivirus* also has a 1.5 Mb genome, in contrast with *Pithoviridae* and other *Pimascovirales*.

Received: February 25, 2023. **Revised:** October 31, 2023. **Accepted:** November 07, 2023

© The Author(s) 2023. Published by Oxford University Press on behalf of Society for Molecular Biology and Evolution.

This is an Open Access article distributed under the terms of the Creative Commons Attribution License (<https://creativecommons.org/licenses/by/4.0/>), which permits unrestricted reuse, distribution, and reproduction in any medium, provided the original work is properly cited.

Open Access

such as *Marseilleviridae* with only 350 kb genomes. In *Nucleocytoviricota*, massive horizontal gene transfers (HGTs) from their host (Moreira and Brochier-Armanet 2008) and gene duplications (Filée and Chandler 2008) have been proposed as the driving force behind their expanded genome size. Another mechanism proposed in *Pandoraviridae* is de novo gene creation from intergenic regions (Legendre et al. 2018). Whatever the main evolutionary process at play, different families of giant viruses exhibit inhomogeneity in their genomes, by having a “creative” part and a “conservative” one. This pattern is revealed by an unequal distribution of core genes, duplicated genes, and genomic rearrangements, preferentially concentrated in one half of the genome (Legendre et al. 2018; Blanca et al. 2020; Christo-Foroux et al. 2020).

Another factor that might shape giant viruses genomes is transposons. For instance, different *Pandoraviridae* are known to harbor miniature inverted transposable elements (MITEs) (Zhang et al. 2018). These nonautonomous class II transposable elements are composed of terminal inverted repeats (TIRs) separated by an internal sequence that lacks the transposase gene. Thus, they rely on an autonomous transposon for transposition (Zhang et al. 2001). Their target sites are often as simple as AT dinucleotides that give rise to target site duplication (TSD) (Ge et al. 2017). In *Pandoravirus salinus*, the transposon probably associated with these MITEs has been found in the genome of the *A. castellanii* cellular host (Sun et al. 2015). The *Pithovirus sibericum* genome also contains many copies of a 140-nucleotide-long palindromic repeated sequence in noncoding regions (Legendre et al. 2014). The nature of these repeated sequences, also found in *Pithovirus massiliensis* (Levasseur et al. 2016), remains unknown. Surprisingly, cedratviruses are completely devoid of such sequences (Andreani et al. 2016).

In this study, we report the genome sequences of 2 new *Pithoviridae* viruses isolated from soil samples (*Cedratvirus borely* and *Cedratvirus plubellavi*), in addition to the recently isolated *Cedratvirus lena* (strain DY0), *Cedratvirus duvanny* (strain DY1), and *Pithovirus mammoth* (strain Yana14) (Alempic et al. 2023). The comparative analysis of these sequenced genomes, complemented with previously published *Pithoviridae* sequences (Legendre et al. 2014; Levasseur et al. 2016; Bertelli et al. 2017; Rodrigues et al. 2018; Jeudy et al. 2020), provides insight into the gene distribution and the evolution of the family. In addition, an in-depth study of pithoviruses genomes reveals that they are highly structured in regions composed of 2 main inverted repeats that have massively colonized their genomes and influenced their evolution.

Results

Pithoviridae Isolation from Soil Samples and Genome Sequencing

We isolated 2 new viruses that belong to 2 species of cedratviruses (*Cedratvirus borely* and *Cedratvirus plubellavi*), both infecting *A. castellanii*, from 2 soil samples located 10 m away in a French park (43°15′34.0″N, 5°22′58.9″E and

43°15′34.3″N, 5°22′59.2″E, respectively). As shown for *Cedratvirus plubellavi* in [supplementary fig. S1, Supplementary Material](#) online, they possess a typical lemon-like *Cedratvirus* morphology with 2 corks, 1 at each apex of the particle. We next sequenced their genomes. In addition, we assembled and annotated the ones of 3 recently reported *Pithoviridae* isolated from various Siberian environments (Alempic et al. 2023), including a *Pithovirus* from frozen soil containing mammoth wool (*Pithovirus mammoth*), a *Cedratvirus* from the Lena river in Yakutsk (*Cedratvirus lena*), and another *Cedratvirus* (*Cedratvirus duvanny*) from a melting ice wedge in the Duvanny Yar permafrost exposure (Table 1). Long-read sequences were available for 3 viruses. They turned out to be essential for the completeness of the *Pithovirus mammoth* assembly, while they only had a minor effect on the *Cedratvirus borely* assembly and no effect at all on the *Cedratvirus plubellavi* one ([supplementary table S1, Supplementary Material](#) online). The 3 genomes were successfully circularized, as shown by the homogeneous long-read coverage along the genomes artificially linearized at 4 equidistant positions ([supplementary fig. S2, Supplementary Material](#) online). It should be noted that the circularity of the *Pithoviridae* genomes has previously been proven by a pulse-field gel electrophoresis experiment on *Cedratvirus kamchatka* DNA (Jeudy et al. 2020).

All included, 12 *Pithoviridae* genome sequences are now available ([supplementary table S2, Supplementary Material](#) online) for a comparative study of the family.

Pithoviridae Phylogeny

To get insight into the *Pithoviridae* family evolution, we next performed a phylogenetic reconstruction of the 12 genomes in addition to the more distantly related *Orpheovirus* (Andreani et al. 2018) and *Hydrivir*, the only complete *Pithoviridae*-like genome assembled from metagenomic data (Rigou et al. 2022). As shown in Fig. 1, *Orpheovirus* and *Hydrivir* are the most divergent pithoviruses and cedratviruses split into 2 well-established clades, and cedratviruses can be further divided into 3 previously defined clades (Jeudy et al. 2020). Although *Hydrivir* and *Orpheovirus* cluster in a well-supported clade, they diverge from each other (average amino acid identity, AAI = 31%) more than cedratviruses from pithoviruses (AAI = 42.2% ± 0.2). In addition, *Hydrivir* and *Orpheovirus* only share 140 hierarchical orthologous groups (HOGs; see [Materials and Methods](#)), as compared with the more than 1,400 genes identified in their respective genomes. This suggests that the group will likely split into better defined clades as new related viruses are added.

Consistent with the phylogeny, the codon usage pattern shows a similar trend, with cedratviruses tightly clustered together, as for pithoviruses, and *Orpheovirus* being the most distant ([supplementary fig. S3, Supplementary Material](#) online). This is in line with the fact that the *Pithoviridae* and *Orpheovirus* infect different laboratory hosts (Andreani et al. 2018).

Within cedratviruses or pithoviruses, genomes are globally collinear despite several rearrangements

Table 1 Genome metrics of sequenced *Pithoviridae* from this study compared with previously published isolates

	Real genome			Without repeats		
	Length (kb)	GC%	Coding density	Length (kb)	GC%	Coding density
<i>Pithovirus mammoth</i>	610	35.8	0.7	469	39.5	0.9
Pithoviruses	637 ± 40.15	35.6 ± 0.13	0.6 ± 0.03	485 ± 0.04	39.5 ± 0.04	0.9 ± 0.02
<i>Cedratvirus borely</i>	570	42.8	0.8	553	42.8	0.8
<i>Cedratvirus plubellavi</i>	568	42.8	0.8	552	42.8	0.9
Cedratviruses clade A	573 ± 10.49	42.8 ± 0.02	0.8 ± 0.01	556 ± 0.01	42.8 ± 0.01	0.8 ± 0.01
<i>Cedratvirus lena</i>	466	40.8	0.8	434	40.7	0.9
<i>Cedratvirus duvanny</i>	472	40.8	0.8	440	40.8	0.9
Cedratviruses clade B	468 ± 3.5	40.7 ± 0.1	0.8 ± 0.02	441	40.7 ± 0.09	0.9 ± 0.01
Cedratviruses clade C	460	43	0.8	445	42.9	0.9

The names of the *Pithoviridae* sequenced in this study are underlined, while the names in bold represent the mean and standard deviation of the group considering all isolates. *Cedratvirus* clades follow the ones defined in Jeudy et al. (2020) and are shown in Fig. 1.

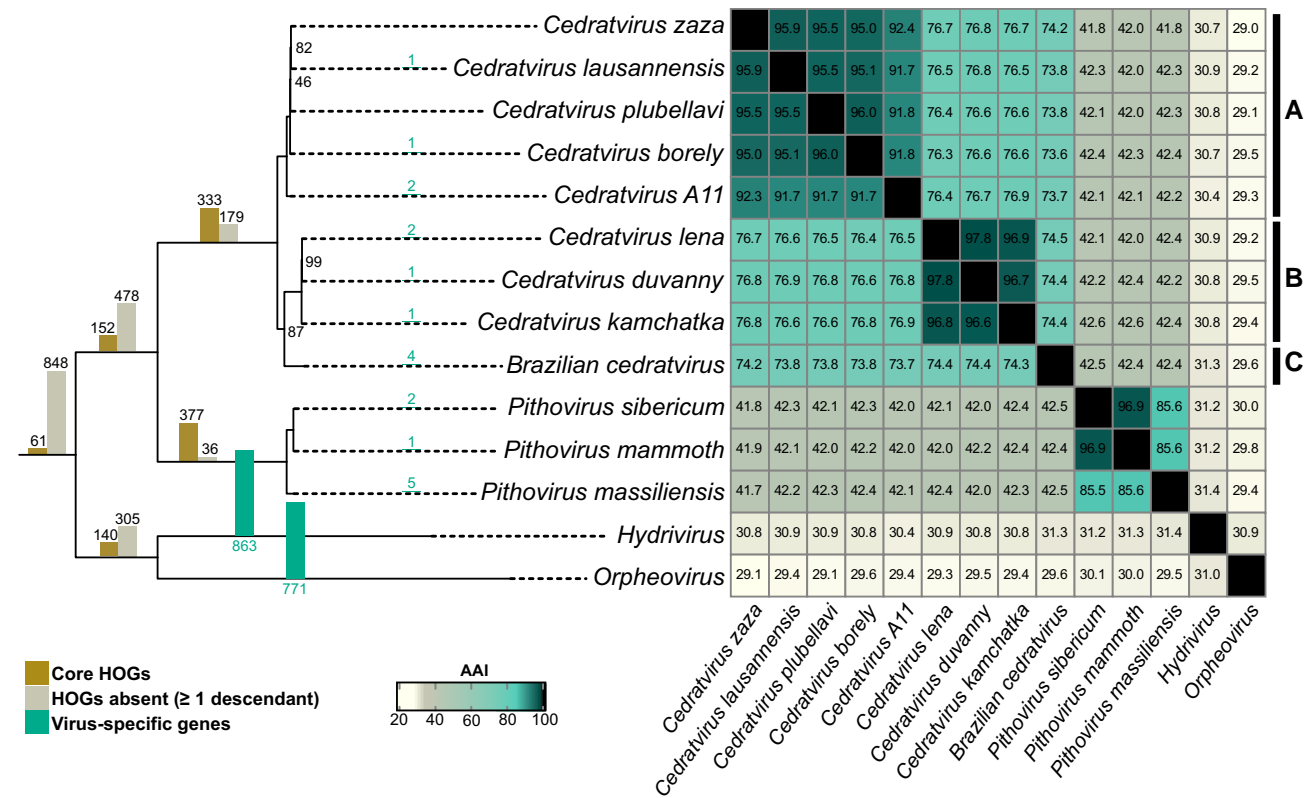


Fig. 1. Phylogeny and AAI of the *Pithoviridae* and their closest relatives. The phylogeny (left) was built from the concatenation of shared single-copy HOGs applying the LG + F + G4 evolutionary model. Bootstrap values are indicated or are 100% otherwise. The bars on each branch represent the number of shared HOGs and other HOGs that were recomputed by OrthoFinder according to this tree. The heatmap (right) shows the AAI between viruses. The rightmost bars (labeled A, B, and C) indicate previously determined *Cedratvirus* clades (Jeudy et al. 2020).

(supplementary fig. S4, Supplementary Material online). *Pithovirus massiliensis* shows 1 major inversion and 1 translocation compared with the 2 other pithoviruses. Both *Cedratvirus kamchatka* and *Brazilian cedratvirus* exhibit many rearrangements compared with clade A.

Heterogeneity within the Genomes of *Pithoviridae*

The comparative genomic studies of other giant virus families previously highlighted a biased evolution of their genomes with a “creative” and a “conservative” part (Legendre

et al. 2018; Blanca et al. 2020). We thus looked for a similar trend in the *Pithoviridae* genomes. As shown in Fig. 2A, core genes are not uniformly distributed along the artificially linearized pithovirus genomes, with a high concentration at one half containing the ATP-dependent DNA ligase. Likewise, core genes are also very scarce in the other half of the cedratvirus genomes. This pattern contrasts with gene duplications that seem to occur in specific hot-spots preferentially located with the accessory genes (Fig. 2B). Altogether, this data show a shared nonuniform architecture of the *Pithoviridae* genomes.

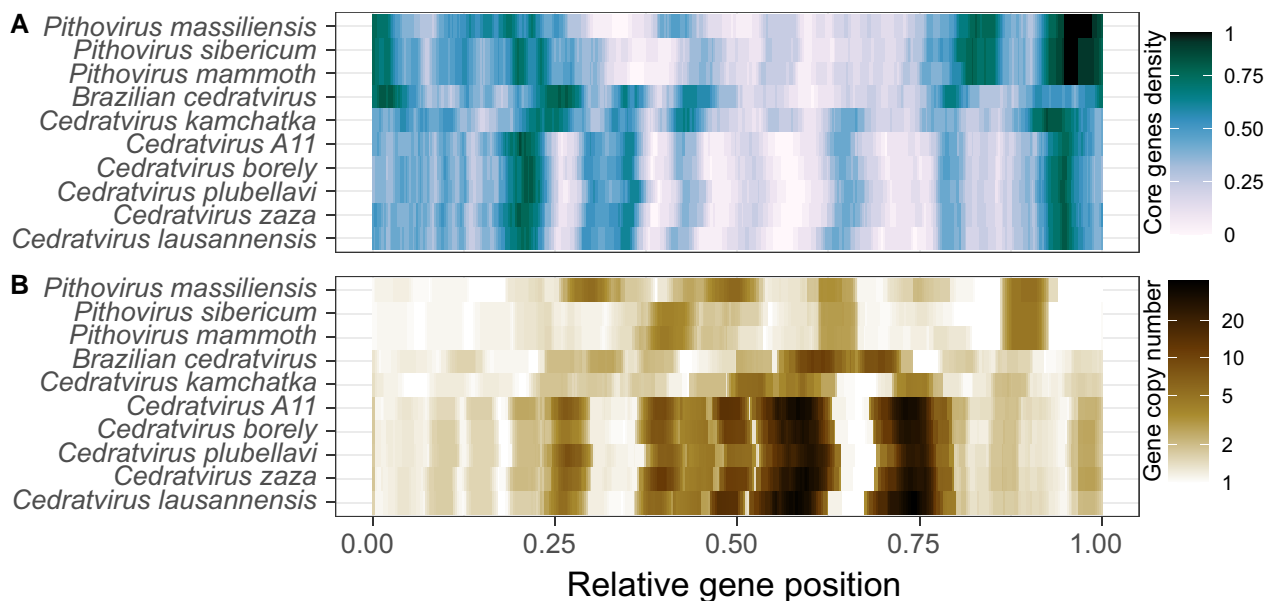


Fig. 2. Nonuniform distribution of core and duplicated genes. A) Density of core genes within a sliding window of 21 ORFs. B) Average gene copy number within the HOGs containing each of the genes of the sliding window.

We next questioned whether *Pithoviridae* DNA was differently epigenetically modified between the “creative” and the “conservative” regions. We analyzed the PacBio data previously generated for *Pithovirus sibericum* and *Cedratvirus kamchatka* (Jeudy et al. 2020) and extracted all positions with interpulse duration (IPD) ratios > 4.5 as potentially modified. We found no significant difference with 0.53 modified bases per kb in the “conservative” region and 0.61 in the “creative” region of *Cedratvirus kamchatka* (χ^2 test P value = 0.34). At this IPD threshold, no *Pithovirus sibericum* nucleotide is predicted to be modified, as previously noticed (Jeudy et al. 2020).

Pithoviridae Are Conservative Compared with Other *Nucleocytoviricota*

We next quantified the *Pithoviridae* core and pan-genomes and compared them with other viral families. The core genome of cedratviruses is made of 333 open reading frames (ORFs) over 100 amino acids (Fig. 3A and B), while the one of the whole *Pithoviridae* family is twice as small with an asymptote at 152 ORFs (Fig. 3B).

The pan-genomes of cedratviruses and *Pithoviridae* (including cedratviruses and pithoviruses) have both reached a plateau (Fig. 3C), suggesting a so-called closed pan-genome. In agreement with this, each new genome brings < 2 new HOGs to the cedratviruses (Fig. 3A). The closedness of the cedratviruses and *Pithoviridae* pan-genomes was confirmed by Heaps’ law models with α estimates of 2 in both cases. Pan-genomes with $\alpha < 1$ are open and $\alpha > 1$ closed. In contrast, *Pandoraviridae* and ranaviruses have open pan-genomes with both α estimates of 0.53. Finally, *Megamimivirinae* and *Marseilleviridae* exhibit a closer pan-genome with α estimates of 1.19 and 1.13, respectively. In other words, *Pithoviridae* appear to be much more conservative (i.e. closer pan-genome) than other

Nucleocytoviricota (Fig. 3C), suggesting that, unlike for *Pandoraviridae*, continuous de novo gene creation might not be a significant process in their evolution (Legendre et al. 2018).

It is worth noting, however, that the phylogenetic breadth of each group has a direct impact on the pan- and core genome trends. According to the lowest AAI within each group (Fig. 3), cedratviruses are more closely related than the other groups (lowest AAI = 73%), whereas *Pithoviridae* contains distant viruses with a lowest AAI value of 42% (Fig. 3). Both phylogenetic groups display a closed pan-genome. In concordance with this apparent conservative evolution, cedratviruses- and pithoviruses-specific genes are mostly shared within their respective genomes, in contrast to *Pandoraviridae* and *Marseilleviridae* that exhibit a much larger fraction of accessory genes within their subclades (supplementary fig. S5, Supplementary Material online). A better sampling of the 2 *Pithoviridae* clades (cedratviruses and pithoviruses) will be needed to confirm the closedness of the family pan-genome.

Gene Duplication and HGT in *Pithoviridae*

Next, we investigated gene duplication as a possible important cause of viral genome gigantism (Filée and Chandler 2008). Gene duplications occurred all along the history of *Pithoviridae*, even during the short divergence time separating the closely related *Pithovirus sibericum* and *Pithovirus mammoth*. They mostly occurred in the vicinity of their original copy with a median distance of 6,872 bp in cedratviruses and 1,575 bp in pithoviruses. Overall, from 14% to 28% (median = 19%) of the *Pithoviridae* genes come from a duplication event (Fig. 4), in line with other *Nucleocytoviricota* such as *Marseilleviridae* (16%), *Pandoraviridae* (15%), and *Megamimivirinae* (14%). Within

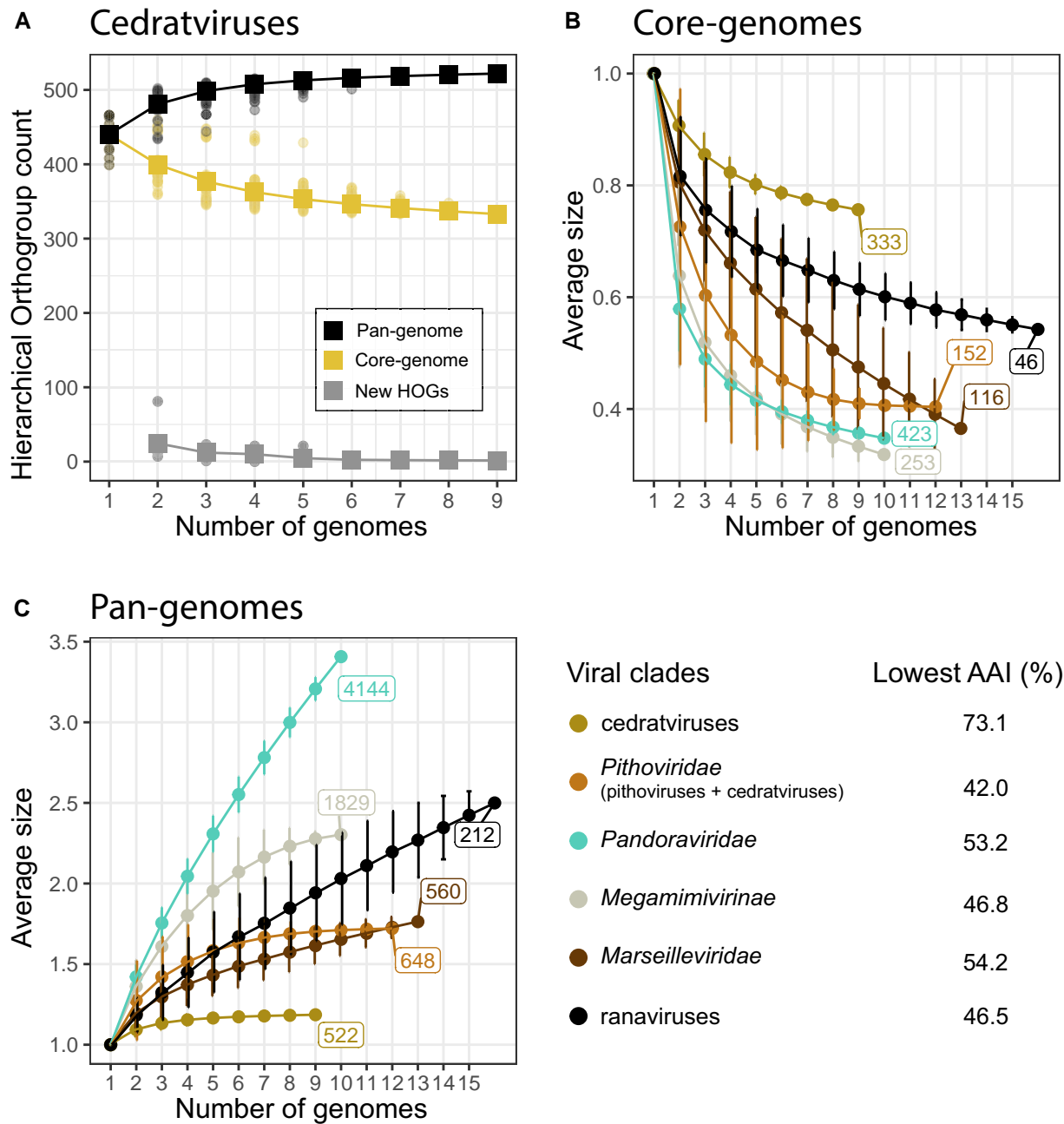


Fig. 3. The core and pan-genomes of *Pithoviridae* and other *Nucleocytoviricota*. A) Pan-genome, core genome, and new HOGs have been estimated for cedratviruses by adding new genomes to a set of previously sequenced genomes in an iterative way (Tettelin et al. 2005). For comparison, the core genome (B) and pan-genome (C) sizes of other *Nucleocytoviricota* have been estimated in the same iterative way. The pan-genome and core genome sizes are defined as the relative size in comparison with their initial mean size. The lowest AAI shown in the legend indicates the AAI of the most distant viruses within the set of genomes used for this analysis.

cedratviruses, gene duplications largely explain genome size variations between clade A and clades B to C, with $27.4 \pm 0.9\%$ in clade A and $18.5 \pm 1.7\%$ in clades B to C (Fig. 4). Consistently, the most duplicated gene, coding for an ankyrin repeat protein, is present in 50 copies in clade A cedratviruses and only 20 copies in clades B to C. Likewise, the related *Orpheovirus* and *Hydrivirus* very large genomes exhibit high rates of gene duplications, with 42% and 27%, respectively (Fig. 4). In contrast, there is a converse pattern in between pithoviruses and cedratviruses, the latter displaying higher

duplication rates while having smaller genomes, suggesting that another factor is at play.

We next investigated HGTs toward our viruses based on the HOG phylogenetic trees complemented with homologous sequences (see Materials and Methods), as a possible source of genome size increase. It turned out that HGTs are far less frequent than gene duplications with a stable fraction of 5% to 7% of the gene content across *Pithoviridae* and in *Orpheovirus* and *Hydrivirus* (Fig. 4).

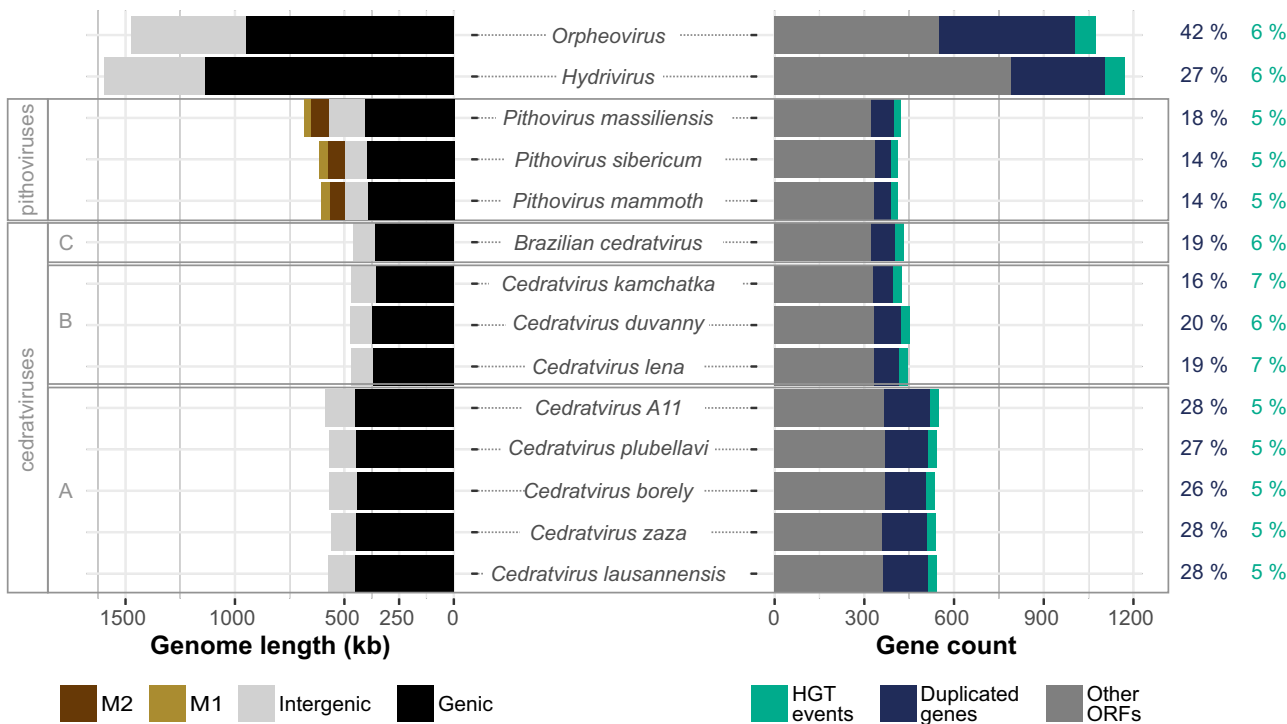


Fig. 4. Genome and gene content statistics of *Pithoviridae* and relatives. The left panel presents the nucleotide content of the different genomes with clade labels on the left (see Fig. 1). M1 and M2 correspond to inverted repeats (see further). The right panel shows their composition in ORFs. The 2 columns on the right show the percentage of genes that arose from a duplication event (left column) and the percentage of HGT events (right column) toward each genome.

The largest proportion of *Pithoviridae* HGTs come from eukaryotes ($42 \pm 2\%$) closely followed by those originating from Bacteria ($41 \pm 3\%$) (supplementary fig. S6, Supplementary Material online). The HGT from Eukaryota do not clearly point to known hosts. Most often, the root of the HGT is ancient, branching before or in between Discosea and Evosea, 2 classes of amoebas (supplementary fig. S6, Supplementary Material online). We also estimate that 10% of the HGT events came from another virus.

Overall, the low rate of HGT in *Pithoviridae* is consistent with the closedness of their pan-genome and thus cannot account for the difference in genome sizes between cedratviruses and pithoviruses, hinting again at a different factor.

Two Types of Inverted Repeats Have Massively Colonized the Genomes of Pithoviruses

Repeat content is another factor that could strongly influence genome size. Indeed, it has been shown that pithoviruses genomes are shaped by intergenic interspersed palindromic repeat sequences (Legendre et al. 2014). These are present in clusters and usually separated by 140 nucleotides (median). After masking these sequences (Fig. 5A and B) from the genomes, we identified additional repeats close to the masked regions (Fig. 5C and D). By running the MUST (Ge et al. 2017) and MITE Tracker (Crescente et al. 2018) tools, we found that both types of repeats were identified as putative MITEs that we referred to as M1 and M2.

We designed a pipeline that defines repeat-rich regions by automatically identifying and clustering repeat sequences (see Materials and methods and supplementary fig. S7, Supplementary Material online). The reference M1 and M2 are palindromic with TIRs of 54 and 47 bp, respectively, and an internal sequence of 37 bp (Fig. 5A and C). The alignment of the extremities of M1 and M2 (and of repeat-rich regions) suggests TA as a putative TSD (supplementary fig. S8, Supplementary Material online). When combined together, the M1 and M2 sequences represent as much as 18.4%, 18.2%, and 16.1% of the genomes of *Pithovirus sibericum*, *Pithovirus mammoth*, and *Pithovirus massiliensis*, respectively (Fig. 4), and 21% to 24% when all kinds of repeats are considered. It is worth noting that when *Pithovirus sibericum* was first discovered, it was estimated that 21% of its genome was covered by repeats (Legendre et al. 2014). This fraction includes both M1 and M2 repeats, although the latter was not identified at the time. Unlike duplicated and core genes (Fig. 3), repeats are not concentrated in specific genomic regions but are uniformly distributed along the pithovirus genomes (Kolmogorov–Smirnov test against uniform distribution P value = 0.6). Our pipeline also provided an extensive description of the structure of the repeated regions resulting in the following rules:

- 1) M2 can never be seen in a repeat region without M1.
- 2) M1 can be seen without M2.
- 3) When several M1 are present in a region, they are always separated by a sequence of about 140 bases, whether M2 is present or not.

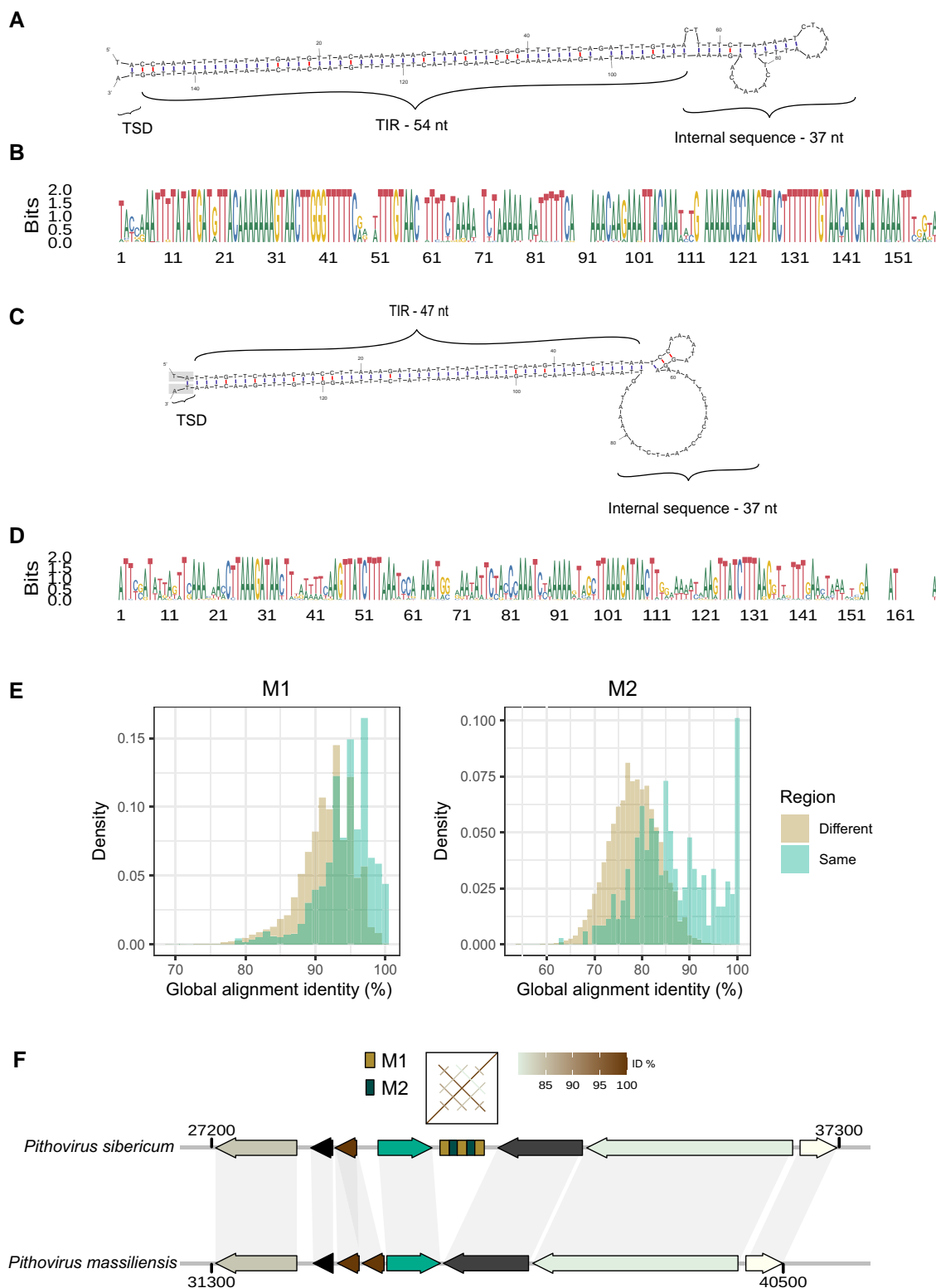


Fig. 5. Main repeats found in pithoviruses. DNA folding structures of the reference sequence for M1 (A) and M2 (C) repeat clusters, respectively. Their free energy ΔG is -79.2 and -65.5 kcal/mol. TSD, target site duplication; TIR, terminal inverted repeat. The TSD highlighted in gray in C) indicates that the dinucleotide is shared between M1 and M2 when the repeats are next to each other. B) and D) are the alignment logos of all the sequences in the clusters of M1 and M2, respectively. E) Pairwise identity percentage in between M1 (left) and M2 (right) repeats retrieved from the same and from distinct regions. The pairwise identity percentages were calculated using the needle tool from the EMBOSS package. Both distributions are significantly different (P values $< 10^{-15}$, Wilcoxon test). F) Example of a repeated region present in *Pithovirus sibericum* but absent from *Pithovirus massiliensis* in a syntenic region of their genomes.

- 4) When several M2 are present in a region, they are separated by M1.

The most common structure of the repeated regions in the 3 pithovirus genomes is (M1-M2){1 to 8 times}-M1. In *Pithovirus sibericum*, M1 is present 515 times and M2 371 times.

For comparison, we also tested RepeatModeler on the *Pithovirus sibericum* genome and identified 4 families of repeats containing 240, 121, 56, and 30 sequences, respectively, covering 25.4% of the genome. As shown by a dotplot of the family consensus sequences (supplementary fig. S9, Supplementary Material online), they partially overlap each other and contain the basic units found by our procedure (M1 and M2). We thus pursued the pithovirus genome analyses with the core units of the repeats identified by our method.

Pithovirus mammoth has a very similar number of regions containing M1 and M2 (supplementary table S3, Supplementary Material online), but the number of M1 or M2 copies per orthologous region is often different. Thus, the differences most often correspond to the extension or contraction of existing repeated regions rather than insertions in a repeat-free region. The extension of existing repeat regions is supported by the fact that repeats from the same region are more similar to each other than repeats from different regions (Fig. 5E; P values $< 10^{-15}$).

Insertion of repeats in repeat-free regions is also necessary to explain the observed high number (> 109) of repeat regions (supplementary table S3, Supplementary Material online). Insertions and/or excisions have happened several times since the divergence of *Pithovirus sibericum* and *Pithovirus massiliensis*, as exemplified by a repeated region in *Pithovirus sibericum* that is absent from the cognate syntenic orthologous region in *Pithovirus massiliensis* (Fig. 5F). This particular example bares no signs of TSD, making transposition mechanism less likely.

M1 and M2 Repeats in Metagenomic Data

We next questioned whether M1 and M2 repeats were present outside the 3 pithoviruses analyzed in this study by screening the nonredundant National Center for Biotechnology Information (NCBI) database (that includes the genome of *A. castellanii*) and metagenomic *Nucleocytoviricota*-assembled sequences, but none were found. As M1 and M2 sequences might be present in metagenomes but lost during the assembly process, we further looked for reads matching these sequences using the NCBI PebbleScout tool (<https://pebblescout.ncbi.nlm.nih.gov/>). We found 28 metagenomic data sets with reads matching M1 or M2 with a PebbleScout score > 70 (supplementary table S4, Supplementary Material online). These correspond to 19 to 1,725 reads and 6 to 368 reads matching M1 and M2, respectively, with a BLASTN E value $< 10^{-10}$. Most of the metagenomic samples correspond to environments for which *Pithoviridae* were previously isolated, namely soil, groundwater, and sediment samples (supplementary table S4, Supplementary Material online).

We then de novo-assembled the 10 data sets with highest density of reads matching M1 or M2 and obtained 363 contigs matching those sequences (BLASTN E value $< 10^{-10}$) among the 16,787,096 assembled contigs. All of them were small, ranging from 211 to 1,091 nt and devoid of ORFs. We also searched for the *Pithovirus sibericum* divergent MCP gene (pv_460) in the assembled metagenomic contigs using TBLASTN and found a highly significant match (E value $< 10^{-22}$) in 9 out of the 10 analyzed data sets. This suggests that the metagenomic contigs matching M1 and M2 might originate from *Pithoviridae*, although we cannot exclude that they belong to other organisms that coexist in the samples.

Furthermore, we found a few *Pithoviridae*-like genomes from metagenomic data that were highly structured by direct repeats (supplementary fig. S10A and B, Supplementary Material online). These constitute 13% of the LCPAC302 pithovirus-like partial genome sequenced from deep-sea sediments (Bäckström et al. 2019). But those repeats have no sequence similarity to M1 or M2. Overall, *Pithoviridae*- and *Pithoviridae*-like genomes are highly diverse in repeat content, ranging from none to almost a quarter of their assembled genomes.

Functional Annotation of Genes Present in Repeat-Rich Regions of Pithoviruses

The M1 and M2 repeats in pithoviruses are palindromic (Fig. 5A and C), such as the MITEs previously identified in pandoraviruses (Sun et al. 2015) and predicted as potential MITEs by MITE searching algorithms. They are also encompassed by potential TSD (supplementary fig. S8, Supplementary Material online), suggesting that they might, at least originally, have integrated the pithovirus ancestor genome through transposition. To explore this possibility, we analyzed the functional annotation of the pithovirus repeat-rich regions, but no transposase could be found in current pithovirus annotations or in M1/M2 containing metagenomic contigs. Instead, we found Gene Ontology (GO) term enrichment for GTP binding and purine nucleoside/ribonucleoside binding (P values for *Pithovirus sibericum* = 0.043, *Pithovirus mammoth* = 0.016, and *Pithovirus massiliensis* = 0.0031).

We next performed a remote homology search from protein structure predictions to identify transposase candidates. AlphaFold models were built for all proteins, followed by structural alignments using Foldseek. Among the folds obtained, 5 had their best matches with transposases or integrases with Foldseek probability > 0.5 (supplementary table S5, Supplementary Material online). Interestingly, all are within repeat-rich regions and part of multiple-copy HOGs. However, the associated Foldseek E values were weak, potentially due to a mild confidence in the AlphaFold models (average pLDDT = 62). In addition, these genes are small (67 amino acids on average) and under weak selective constraints, with nonsynonymous substitution rate (dN)/synonymous substitution rate (dS) ratios of 0.98 ± 0.7 . This suggests that if these transposase-related genes were indeed involved in M1/

M2 transposition, they are probably inactive and undergoing pseudogenization.

We next pursued the strategy of structural homology search to increase *Pithovirus sibericum* functional annotation. This resulted in 37 genes with a better functional annotation (supplementary table S6, Supplementary Material online), of which 9 are located in repeat-rich regions. One of those, pv_445, is a crossover junction endonuclease RuvC-like that is absent in cedratviruses. By aligning the pv_445 model with the *fowlpox virus* structural homolog (Li et al. 2020), we identified the DDE active site and other residues important for DNA binding and cleavage (supplementary fig. S11, Supplementary Material online). One could hypothesize that this protein is involved in homologous recombination as a repeat expansion factor. Finally, the Foldseek alignments revealed a SbcCD subunit D Nuclease (supplementary table S6, Supplementary Material online) that cleaves DNA hairpin structures. Hairpins are dense in repeats, which may increase the instability of those regions. This gene, in conjunction with the DNA double-strand break repair ATPase (pv_215 in *Pithovirus sibericum*), could possibly also be a part of the machinery helping the spread of M1 and M2 sequences.

Pithovirus Repeat-Rich Regions Are Hotspots of Genetic Variability

As repeats constitute a large proportion of pithoviruses genomes, we further investigated the genes located in those regions from an evolutionary perspective. Although HGTs are not abundant in pithoviruses (Fig. 4), they are slightly but significantly enriched in repeat regions: 12.4% within versus 4.7% outside (χ^2 test P value = 1.7×10^{-7} and individual P values of 0.002, 0.007, and 0.001 in *Pithovirus sibericum*, *Pithovirus massiliensis*, and *Pithovirus mammoth*, respectively).

We also estimated the ancestry of the genes present within these regions compared with other regions. This was performed considering the last common ancestor of all species within each HOG. From that, we observed a significant trend (Cochran–Armitage test P value = 2.6×10^{-3}) whereby newly acquired genes appeared more frequent than ancestral genes in these regions (Fig. 6A). In other words, repeated regions are more prone to gene novelty.

The rates of mutation in repeat-rich versus repeat-free regions were compared using orthologous genes. We found that genes located in repeat-rich regions tended to have higher mutation rates for both synonymous (P value = 5.2×10^{-10}) and nonsynonymous (P value = 1.1×10^{-13}) positions (Fig. 6B). All trends are confirmed when considering each individual genome (maximum P value = 7.3×10^{-4}). In addition, the genes within repeat-rich regions also exhibit higher dN/dS values and thus are less evolutionarily constrained (Fig. 6B, P value = 3.1×10^{-5} and maximum P value for individual genomes = 0.027).

Finally, we investigated the frequency of genomic rearrangements located in repeat-rich compared with repeat-

free regions. We took advantage of the fact that 2 pithoviruses (*Pithovirus sibericum* and *Pithovirus mammoth*) were sequenced using long reads and exhibited mostly colinear genomes. We manually inspected orthologous regions of these 2 viruses to spot potential rearrangement and mutational events. Again, we found that repeat-rich regions were highly enriched in several types of rearrangements compared with repeat-free regions. This includes insertions/deletions, inversions, duplications, and substitutions affecting genes, accounting for a total 28 events in repeat-rich regions for only 13 in repeat-free regions (χ^2 P value = 1.42×10^{-11} ; supplementary table S7, Supplementary Material online).

Altogether, these various results establish that pithovirus repeat-rich regions are hotspots of genetic novelty and undergo relaxed evolutionary constraints.

Discussion

Here, we reported the isolation from soil samples and genome sequencing of 2 cedratviruses (*Cedratvirus borely* and *Cedratvirus plubellavi*). We also assembled and annotated the genome of *Pithovirus mammoth* recently isolated from 27,000-yr-old permafrost, of a *Cedratvirus* from fresh water (*Cedratvirus lena*) and another one from melting ice (*Cedratvirus duvanny*) (Alempic et al. 2023). Along with previously described *Pithoviridae*, mostly originating from permafrost (Legendre et al. 2014) and sewage water (Levasseur et al. 2016; Bertelli et al. 2017; Silva et al. 2018), these new isolates confirm the ubiquity of this viral family, members of which are present within various aquatic and soil environments. This is also consistent with recent metagenomic surveys exhibiting the presence of *Pithoviridae* in permafrost, forest soils, and deep-sea sediments (Bäckström et al. 2019; Rigou et al. 2022).

These 5 additional sequenced strains were combined to 7 previously published genomes to perform a thorough comparative analysis of the *Pithoviridae* family, revealing the organization of their circular genomes. We have found that repeat content is highly diverse within this family. This directly impacts the strategies employed for genome assembly. While addition of long reads only had a limited benefit over short-read only assemblies of cedratviruses, it has a drastic effect on the genome completeness of highly repeated pithoviruses genomes (supplementary table S1, Supplementary Material online). This recently prompted some authors to employ long reads only as a cost-effective strategy for complete genome assembly of giant viruses, including a *Pithovirus* (Hikida et al. 2023).

In all *Pithoviridae* assemblies, we found that their genes are broadly distributed in 2 distinct regions, 1 enriched in core genes and the other in gene duplications (Fig. 2). This type of nonuniform genome partition with a “creative” and a conserved region is reminiscent of what has been observed in *Marseilleviridae* (Blanca et al. 2020), a viral family belonging to the same order (*Pimascovirales*) and whose genomes are also circular. However, the 2 regions are more clearly defined in *Marseilleviridae*, where

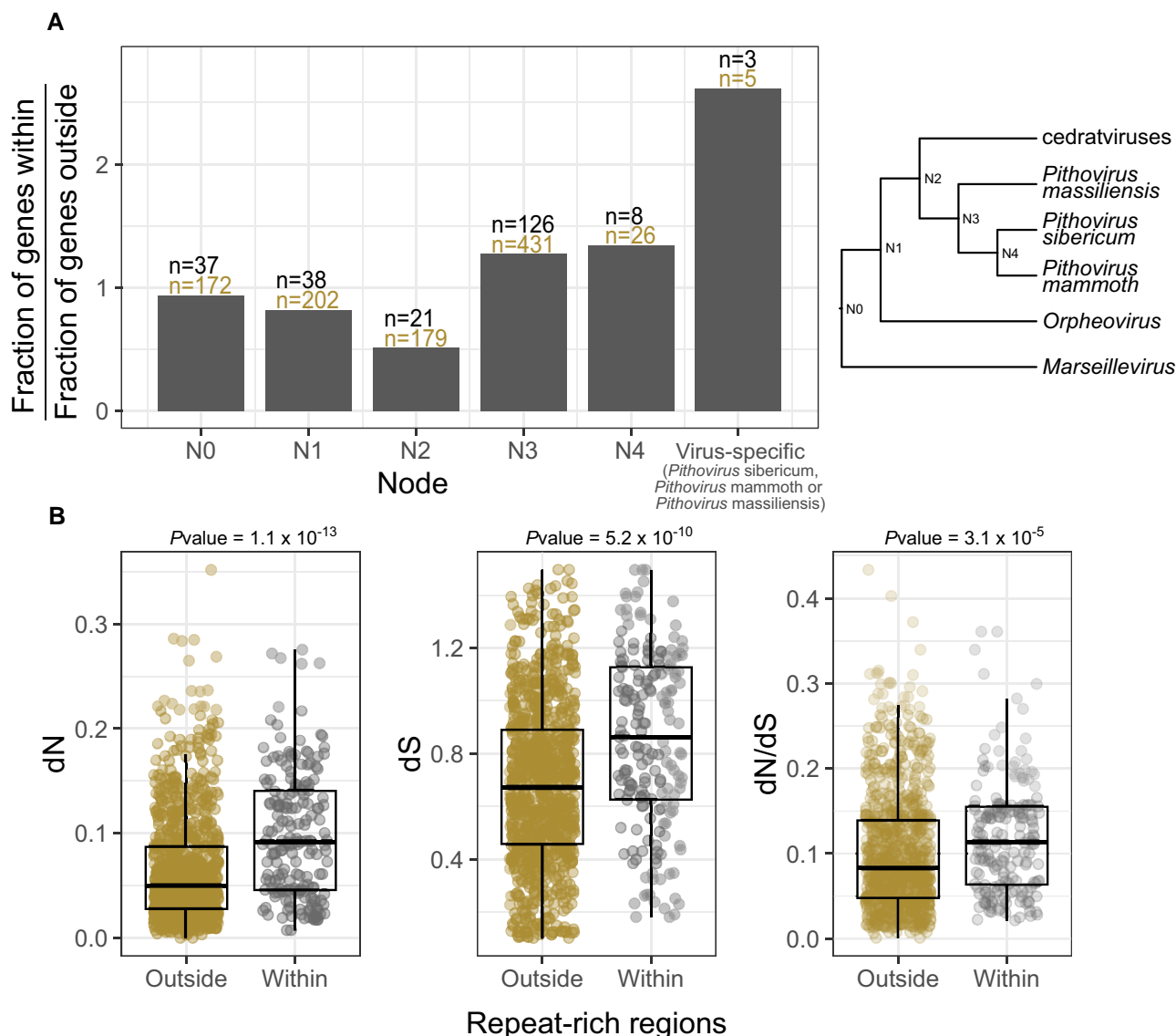


Fig. 6. Evolution of ORFs within and outside repeat-rich regions. A) Ancestry of genes within and outside repeat-rich regions. The ancestry of each gene was estimated considering the last common ancestor of the species present in the cognate HOG. Nodes are ordered from the most ancient to the most recent, as shown in the cladogram next to the plot. B) dN, dS, and dN/dS values for all genes within (gray) or outside (brown) repeat-rich regions detected by our pipeline. P values were calculated using Wilcoxon rank tests.

duplications and accessory genes are evenly dispersed in the “creative” region, while they occur in hotspots in *Pithoviridae* (Fig. 2). Other viral families, which only share a handful of genes (Mönttinen et al. 2021) and have various virion morphology and genome organization (linear or circular), also exhibit this nonuniform distribution of their genes. In *Poxviridae*, for instance, core genes are concentrated in the central part of the genome, while accessory genes, mostly involved in host–virus interactions, are located at the genome termini (Senkevich et al. 2021). It has been proposed that this accessory partition is a hotspot of frequent gene loss and gain through HGTs (Senkevich et al. 2021), but the few HGT identified in *Pithoviridae* does not support this model. In *Pandoraviridae*, core and essential genes, and those whose proteins are identified in the viral particle, are mostly

localized in the left part of the genome, while accessory genes are located on the right part (Legendre et al. 2018; Bisio et al. 2023). This likely reflects ongoing genome increase involving de novo gene creation (Legendre et al. 2018) and accelerated gene duplications (Bisio et al. 2023). One could also hypothesize that the partitioning of the genomes is linked to a global epigenetic regulation of gene expression. However, in this work, we found no difference in modified base densities between the 2 regions in *Pithoviridae*, which is consistent with the uniform distribution of known methylated motifs in giant virus genomes (Jeudy et al. 2020). Transcriptome analyses of the *Pithoviridae* would be needed to determine whether gene expression profiles are globally different in these large genomic regions. Another factor that might explain the dichotomous partitioning of the *Pithoviridae* genomes is

DNA compaction. But while virally encoded histones have been found in other *Pimascovirales*, namely *Marseilleviridae* (Thomas et al. 2011; Liu et al. 2021), our thorough gene annotation of isolated *Pithoviridae* has not identified such proteins yet. To explore this hypothesis, global 3D structure of the different genomic regions remains to be examined by chromosome conformation capture experiments.

Even though *Pithoviridae* genomes are conservative, the cedratviruses and pithoviruses clades exhibit large differences in genome sizes correlated with their repeat contents. The pipeline we designed to study them identified 2 repeated units in pithoviruses, referred to as M1 and M2. Those repeats share some features with MITEs, such as TIRs (Fig. 5), size, and putative TSD (supplementary fig. S8, Supplementary Material online). They are frequently organized in (M1-M2){*n* times}-M1 repeated patterns, suggesting that M1 and M2 mostly move together. However, the fact that M1 can be seen without M2, and is also more frequent (supplementary table S3, Supplementary Material online), suggests that they were once independent. It is not uncommon for MITEs to transpose alongside another MITE, like in the rice (*Oryza sativa*) genome where this event occurred several times (Tarchini et al. 2000) and where 11% of MITEs exist in multimers (Jiang and Wessler 2001). If M1 and M2 are genuine MITEs, they have to rely on an autonomous transposon for transposition. In *Pandoraviridae*, the *submariner* MITEs that colonized their genomes are related to a transposon present in their *A. castellanii* host genome (Sun et al. 2015; Zhang et al. 2018). We did not find transposons related to M1 and M2 in the available *A. castellanii* genome sequences, and current pithovirus annotations show no sign of transposase. However, a recent study has found a putative transposase in the *Pithovirus sibericum* and *Pithovirus massiliensis* genomes, thanks to profile-based remote homology searches (Queiroz et al. 2023). The transposase found in *Pithovirus sibericum* is present within a repeat-rich region, while in *Pithovirus massiliensis*, it is adjacent to one. Those genes are thus candidates for explaining repeat invasion, but the fact that they are core genes, shared with all cedratviruses, makes it less likely. Here, we used structure-based remote homology searches thanks to AlphaFold models coupled with Foldseek searches to further improve pithoviruses functional annotations. In doing so, we found candidate transposases that are systematically present in repeat-rich regions and potentially undergoing pseudogenization (supplementary table S5, Supplementary Material online).

M1 and M2 repeats also share the characteristics of satellite DNA repeats, with a variable number of repeated units between closely related species and a similar size range (Thakur et al. 2021). Furthermore, the pattern of higher sequence identity of repeats within the same regions (Fig. 5E) is reminiscent of the homogenization of repeat copies through concerted evolution (Thakur et al. 2021). This is particularly true for M1, but less so for M2 (supplementary fig. S12, Supplementary Material online).

Thus, pithoviruses repeats might have also multiplied within genomes through recombination events rather than transposition, like in mice where it has been shown to increase the number of palindromic sequences (Zhou et al. 2001). In line with this hypothesis, our structure-based remote homology searches have revealed 2 proteins that could be involved in this process. The first one, pv_445 in *Pithovirus sibericum*, is probably a RuvC-like crossover junction endonuclease (supplementary table S6, Supplementary Material online). These proteins are involved in Holliday junction resolution formed by concatemers in *Nucleocyotvira cota* with linear genomes such as *Poxviridae* (Culyba et al. 2009). They are also involved in the cleavage of cruciform (4-way junction) formed by inverted repeats, such as M1 and M2, to serve as intermediates in homologous recombination (Bowater et al. 2022). The second candidate, pv_159 in *Pithovirus sibericum*, is a probable SbcCD subunit D nuclease (supplementary table S6, Supplementary Material online). These proteins, in addition to the DNA topoisomerase II (Froelich-Ammon et al. 1994) also found in *Pithoviridae*, are involved in the structural maintenance of chromosomes that cleave DNA hairpins and lead to homologous recombination (Connelly et al. 1998). The DNA breaks formed by these enzymes might also lead to the translocation of pithoviruses repeats into repeat-free regions.

It has been proposed that transposable elements can behave as seeds for the formation of satellite DNA (Meštrović et al. 2015; Garrido-Ramos 2017). The following scenario can thus be hypothesized for the invasion of pithoviruses genomes by repeats: initial transposition that occurred in the pithoviruses ancestor in 1 or several locations, probably followed by the inactivation of the transposase, and expansion by recombination as well as translocation into regions without repeats. The primo-invasion followed by drastic expansion occurred after the *Pithovirus/Cedratvirus* divergence. Was this the result of an explosive event or that of a gradual invasion remains to be determined. More deeply branching pithoviruses would be needed to settle this question. Interestingly, comparison of the *Pithovirus sibericum* and *Pithovirus massiliensis* genomes shows that the excision/insertion of their repeats has been ongoing since the 2 species diverged, more than 30,000 yr ago (Legendre et al. 2014; Levasseur et al. 2016).

If repeat-rich regions constitute a large fraction of pithovirus genomes, covering as much as a quarter of their genomes, they are also the source of genetic innovations. By comparing genes localized in repeat-rich regions with those in other regions, we found that they are more divergent and less evolutionary constrained (Fig. 6). We also found that repeat-rich regions are prone to gene capture of cellular and viral origins and undergo many genomic rearrangements. One could hypothesize that the high conservation of repeat sequences triggers genomic recombination and gene exchange between coinfecting viral strains. As previously stated, our comparative analysis of the *Pithoviridae* family shows that they are conservative

compared with other giant virus families. These genomic islands might thus provide an opportunity for them to promote genetic diversity and raw genetic material for evolution to work on.

Materials and Methods

Isolation of Cedratviruses

Cedratvirus borely and *Cedratvirus plubellavi* were isolated in February 2017 from muddy soil samples from Marseilles, France (Parc Borély). The isolation and cloning of viruses were performed as previously described (Alempic et al. 2023). Briefly, mud was collected in sterile 50-mL Falcon tubes and several grams of this soil was resuspended, centrifuged, and deposited on a Petri dish with 5,000 *A. castellanii* (Douglas) Neff (ATCC 30010) cells/cm² growing on PPYG medium (for peptone, yeast extract, and glucose). On the contrary of Alempic et al. (2023), this step did not require fungizone. After 3 days, signs of a giant virus infection were looked for under the light microscope and amoeba cells were transferred to T25 cell culture flasks with *A. castellanii* cells in PPYG medium with ampicillin, chloramphenicol, and kanamycin antibiotics and fungizone. After 2 to 3 days, when an ongoing viral infection was visible, cloning was performed by infecting a 6-well plate with 100,000 cells/cm² with an MOI of 2. After 1 h and 30 min, the wells were washed 50 times with 2 mL of PPYG. Cells were then scraped and transferred to a 12-well plate with 1 mL of PPYG in each well. Serial dilutions by 1/2 were performed. From the 6th to 8th well, 0.4 µL were transferred to a 24-well plate with PPYG medium. Wells with only 1 cell, as observed under the light microscope, were added with 200 cells then with 100,000 cells after 3 days. One week later, viruses were produced in T25 flasks with *A. castellanii* and purified on a cesium chloride gradient.

Genome Sequencing and Assembly

250 ng of DNA of *Pithovirus mammoth* was sequenced by Oxford Nanopore flowcell version R9.4.1 with the 1D native DNA barcoding protocol and by Illumina MiSeq. Long reads were basecalled by guppy v 2.1.3. Sequence data were assembled using a combination of short and long reads over 40 kb by Unicycler v. 0.4.8 (Wick et al. 2017). The *Cedratvirus borely* genome was sequenced using Illumina MiSeq, assembled using SPAdes (version 3.9.1 and the “careful” option), scaffolded using SSPACE (SSPACE-LongRead v1.1) (Boetzer and Pirovano 2014) with Oxford Nanopore long reads (same protocol as above), and polished with Illumina reads using pilon v. 1.24. The *Cedratvirus plubellavi* genome was assembled using SPAdes (v 3.9.0) with Illumina MiSeq reads and Oxford Nanopore reads (option “careful”). Finally, the genomes of *Cedratvirus lena* and *Cedratvirus duvanny* were sequenced using Illumina MiSeq and NovaSeq technologies. *Cedratvirus lena* was assembled after removing reads mapped to a contaminant *Pandoravirus* using Bowtie2.

Cedratvirus lena and *Cedratvirus duvanny* reads were trimmed by BBDuk (sourceforge.net/projects/bbmap/) and assembled using SPAdes v 3.14 (Prjibelski et al. 2020) with options “careful” and k = 15, 17, 19, 21, 29, 33, 41, 55, 63, 71, 91, 101, 115. The scaffolding was then performed by RaGOO (Alonge et al. 2019) using *Cedratvirus kamchatka* as template. The genome of *Pithovirus sibericum* was reassembled using PacBio long reads over 500 bp from Jeudy et al. (2020) with Unicycler v 0.5.0. A total of 100,000 sampled short-read pairs from Legendre et al. (2014) were trimmed with BBDuk and aligned to the genome with Bowtie2 with option “no-discordant”. Polishing was done by pilon v. 1.24.

The 10 metagenomic data sets with the highest density of reads matching the M1 or M2 repeats (supplementary table S4, Supplementary Material online) were retrieved from the Sequence Read Archive (SRA) archive and cleaned using BBDuk with the following parameters: “ref = adapters ktrim = r k = 23 min = 11 hdist = 1 tpe tbo”. The data sets were then individually assembled using megahit (v 1.1.3) with default parameters.

The 3 pithoviruses and the 9 cedratviruses genomic sequences (accessions in supplementary table S2A and B, Supplementary Material online) were then artificially linearized to start at the same position for comparative analyses. *Cedratvirus A11* and *Pithovirus sibericum* were used as reference to linearize cedratviruses and pithoviruses. All genomes were aligned with progressiveMauve and visualized with Mauve to identify the corresponding starting positions in other *Pithoviridae*. Their genomes were then cut and swapped at this reference position. The genome of *Brazilian cedratvirus*, having undergone several genomic rearrangements, was then reverse complemented to better fit the genome structure of other cedratviruses (supplementary fig. S4, Supplementary Material online).

Genome Annotation

For functional annotation, genes were predicted using GeneMark (Besemer et al. 2001) with option –virus. ORFs over 50 amino acids were kept for publication, and ORFs over 100 amino acids were used for core and pan-genome comparative analyses.

ORFs were annotated using InterProScan (v5.39-77.0, databases PANTHER-14.1, Pfam-32.0, ProDom-2006.1, ProSitePatterns-2019_01, ProSiteProfiles-2019_01, SMART-7.1, TIGRFAM-15.0) (Jones et al. 2014) and CDsearch (Conserved Domain Database) (Lu et al. 2020) with default options. We also searched for viral specific functions using hmmsearch on the virus orthologous group database (<https://vogdb.org/>) from November 2022 with an *E* value cutoff of 10^{−5}. ORFs were compared with the nr and SwissProt databases using BLASTP (Altschul et al. 1990) and *E* values cutoff of 10^{−2}. Transmembrane domains were identified with Phobius (Käll et al. 2004).

For further improving the functional annotation, we generated AlphaFold2 (Jumper et al. 2021) models of the proteins of all 3 pithoviruses using the ColabFold

(Mirdita et al. 2022) pipeline version 1.52. Multiple sequence alignments were computed using MMSeqs2 (Steinegger and Söding 2017) with default parameters and the UniRef30 (version 2202), pdb70 (version 220313), and envDB (version 202108) databases. Structure prediction was processed with default parameters, automatic number of recycles (up to 20), no templates, and no relax. For each protein, only the top ranked model (by pTM) was selected for the next steps. We next used Foldseek (van Kempen et al. 2023) through API to search the AlphaFold-SwissProt, AlphaFold-Proteome, and PDB100 databases from July 2023. For final annotations in *Pithovirus sibericum* (supplementary table S6, Supplementary Material online), only matches with over 50% of subject coverage, an *E* value below 0.01, and a probability over 50% were considered. The consistency in between the function of the best Foldseek matches was checked, and functional annotation was done manually.

Two-way AAI were calculated for all pairs of genomes by the package *enveomics* (Rodriguez-R and Konstantinidis 2016) and options `-id 15 -L 0.4`.

Relative synonymous codon usage was calculated using an in-house script, *genome_metrics.py*, for fast genome-wide analysis relying on Biopython (Cock et al. 2009). Given an amino acid *a* and a codon *c*, we applied the following formula:

$$\text{RSCU}_a = \frac{\text{counts of } c \times \text{number of synonyms in the genetic code}}{\text{counts of } a}$$

The heatmap and multidimensional scaling were done on the RSCU calculated on the whole genome (i.e. treating all the codons in the genome at once) excluding stop codons and tryptophan codons.

Computation of Orthologous Gene Groups and Phylogeny

A phylogenetic tree was computed by OrthoFinder (v2.5.4) (Emms and Kelly 2019) using all available *Pithoviridae* genomes in addition to the *Orpheovirus* (Andreani et al. 2018), *Hydrivir* (Rigou et al. 2022), and *Marseillevirus* genomes (supplementary table S2, Supplementary Material online). The tree was then rooted using the distantly related *Marseillevirus* (Boyer et al. 2009) as an outgroup. HOGs were then determined by OrthoFinder (v2.5.4) using this rooted tree. A final phylogeny was inferred on the concatenated alignment of single-copy core HOGs by IQ-TREE (Nguyen et al. 2015) with the LG + F + G4 model and options `-bb 5,000 -bi 200`.

The distribution of core genes and duplications along the *Pithoviridae* genomes were evaluated through a sliding window of 21 genes. The genomes were considered circular; meaning that, at the extremities of the artificially linearized genomes, the window would span across the other end of the genome.

Selection pressure on genes was estimated by the ratios of dN to dS, calculated by *codeml* of the PAML v4.9 package (Yang 1997). All pairs of single-copy orthologues as defined by OrthoFinder were retrieved and aligned with T-Coffee (Notredame et al. 2000). *Codeml* was given the sequence pair alignments, and the resulting dN/dS ratio was considered only if $dS < 1.5$, $dS > 0.1$, and $dN/dS < 10$. Later, the dN and dS values for each gene were estimated as the mean of all value calculated on gene pairs.

Estimation of the Core and Pan-genomes of Cedratviruses

Core/pan-genome sizes were calculated on HOGs at the root node. Genomes were iteratively added with all possible combinations to simulate a data set with 1 to 9 genomes. We used the presence/absence matrix of HOGs instead of gene counts as in the original method (Tettelin et al. 2005). Data were processed using R (v4.04 (R Core Team 2021)). First, OrthoFinder data were transformed into a numeric matrix with the function “HOG2dP” taking as arguments *Phylogenetic_Hierarchical_Orthogroups/Nx.tsv* and *Orthogroups_UnassignedGenes.tsv* file locations. Next, the simulated data sets were processed by functions “get_core_pan_new_info_Real” for cedratviruses (Fig. 3A) and with function “get_core_pan_info” for the comparative analyses with normalized genome sizes (Fig. 3B and C). In addition to this method, the micropan package (Snipen and Liland 2015) was used to estimate the closedness/openness of the different pan-genomes applying Heaps’ law with option `n.perm = 1,000`. Pan-genomes are considered open when the estimated α parameter < 1 and closed otherwise.

For comparison, the ORF predictions, orthology analyses, and core/pan-genome estimations were performed on other viral families: *Pandoraviridae* (supplementary table S2C, Supplementary Material online), *Marseilleviridae* (supplementary table S2D, Supplementary Material online), *ranaviruses* (supplementary table S2E, Supplementary Material online), and *Megavirinae* (supplementary table S2F, Supplementary Material online). The outgroups used were respectively *Mollivirus sibericum*, *Ambystoma tigrinum virus*, *Red seabream iridovirus*, and *Chrysochromulina ericina virus*.

Identification of HGTs

HGTs were identified based on phylogenetic trees of each HOG complemented with homologous sequences that were retrieved using a 2-step procedure. First, the sequences of each HOG were aligned using DIAMOND BLASTP (Buchfink et al. 2015) against the RefSeq database from March 2019 (O’Leary et al. 2016) with an *E* value threshold of 10^{-5} , keeping only matches covering more than 50% of the query. Up to 10 matches per domain (Bacteria, Archaea, Eukaryota, and Viruses) were kept for each query, and CD-hit was applied on the retrieved sequences. Secondly, the resulting sequences were queried again against the RefSeq using DIAMOND with the same *E* value threshold. A maximum of 2 proteins per domain,

whose matches covered more than 80% of the query, were kept at this point. The HOGs and selected sequences from the first and second rounds were aligned using MAFFT v7.475 (Katoh and Standley 2013), and phylogenetic trees were built using IQ-TREE with options -bb 1,000 -bi 200 -m TEST. Each resulting phylogenetic tree was rooted by mad v2.2 (Tria et al. 2017). Trees were finally visually inspected and HGT events counted when 1 or several *Pithoviridae* genes were within a bacterial, eukaryotic, archaeal, or different viral clade.

Detection and Classification of Genomic Repeats

A pipeline was developed to retrieve repeat-rich regions and map individual repeats from pithovirus genomes. The steps were (i) genome-wide alignment, (ii) flattened dotplot calculation, (iii) repeat-rich region mapping, (iv) individual repeat retrieval, and (v) repeat clustering.

- 1) Genomes were aligned against themselves by BLASTN with an E value threshold of 10^{-10} .
- 2) For each position of the genome, the number of times it was aligned was counted resulting in a vector (y), similar to a flattened dotplot.
- 3) A smooth vector (y_s s) was first estimated by sliding mean filtering with a window size of 500 nt. A detection threshold (τ) was calculated as $\tau = \bar{y}_s * \text{sensitivity}^{-1}$, with a sensitivity coefficient set to 2.5. Repeat-rich regions were detected by comparing the vector y_s with τ . Repeat-rich regions were defined as regions where y_s is above the threshold τ . Each region's start and stop are thus the positions of intersections of y_s and τ .
- 4) For each previously detected region, individual repeats were extracted using a smoothed derivative of y . Smoothing was applied before and after the derivation, this time with a window size of 20 nt. Then, the absolute value was taken in order to obtain the vector $|y_s|$. Then, the local maxima were considered as repeat delimitations if above a cutoff set to 10.
- 5) Repeats are globally aligned to each other by needle of the EMBOSS suite (Rice et al. 2000). They are then ordered according to the mean distance (100—needle identity percentage) to their 10 closest neighbors. The first sequence becomes a reference sequence. Then, sequences are clustered together if they are at least 70% identical to a reference or they become themselves a reference. Finally, clusters are merged together if over half of their respective sequences are at least 70% identical. For visual inspection to infer repeat types and similarity in between clusters, a matrix of dotplots presenting the alignments of reference sequences is drawn.

For an in-depth analysis of pithovirus repeats, the sequences from the largest cluster of repeats (M1) were aligned with MAFFT and trimmed according to the position of the aligned terminal “TA”. The reference sequence

(see step 5) of M1 and M2 were folded by mFold (Zuker 2003). To retrieve divergent M1 and M2 clusters, the dotplots of reference sequences were visually inspected. Reference sequences aligned to the reference of M1 or M2 clusters were annotated as M1- or M2-like (example given by cluster 3 in step 5; [supplementary fig. S7, Supplementary Material](#) online).

MUST v2-4-002 (Ge et al. 2017) and MITE Tracker (Crescente et al. 2018) were used to infer the nature of the repeats.

For comparison, we also ran RepeatModeler v2.0.4 on the genome of *Pithovirus sibericum*.

Repeat and Adjacent Sequence Similarity

To compare the similarity of M1 or M2 within the same or different regions, we used the percentage of identity calculated from pairwise global alignments by needle in step 5 of the described pipeline. To compare similar numbers of pairs, we randomly subsampled pairs of repeats originating from different repeat-rich regions to match the number of pairs of repeats originating from the same region. The operation was done several times, and the results were always comparable with the results in [Fig. 5](#).

Statistics of Genes within Repeat-Rich Regions

The repeat detection pipeline was used with a smoothing window size of 4,000 nt (3) to define repeat-rich regions. Bedtools intersect was used to reveal the genes that were within repeat-rich regions. GO term enrichment analyses were performed on those genes by extracting the GO terms of the nonoverlapping protein domains predicted by InterProScan in the 3 genomes. The topGO package of R was used to test the significantly enriched molecular functions in repeat-rich regions versus outside those regions through a Fisher test.

Supplementary Material

[Supplementary material](#) is available at *Molecular Biology and Evolution* online.

Acknowledgments

This work was supported by Agence Nationale de la Recherche grants ANR-22-CE12-0041 to M.L. and ANR-10-INBS-09-08 to J.-M.C. and CNRS Projet de Recherche Conjoint (PRC) grant PRC1484-2018 to C.A. S.R. was supported by a doctoral fellowship obtained from Aix-Marseille University. We thank the PACA Bioinfo platform for computing support and the GENCI-IDRIS for the GPU HPC resources used for AlphaFold predictions (grant 2022-AD011013526). We also thank Hugo Bisio for carefully reading the manuscript, as well as Bernard La Scola and Julien Andreani for giving access to the raw sequencing data of *Brazilian cedratvirus* and Victória Queiroz for providing additional gene annotations.

Data Availability

Genome sequences and annotations of the following 5 *Pithoviridae* have been deposited to GenBank: *Cedratvirus borely* (OQ413575), *Cedratvirus plubellavi* (OQ413576), *Cedratvirus lena* (OQ413577, OQ413578, OQ413579, OQ413580), *Cedratvirus duvanny* (OQ413581), and *Pithovirus mammoth* (OQ413582). R functions for pan- and core genome analysis as well as HOGs are available for download: <https://doi.org/10.6084/m9.figshare.23913051>, together with rooted trees and the final HGT analysis results. Additional in-house scripts are also provided here. The code for pithovirus repeat detection and clustering is available at <https://src.koda.cnrs.fr/igs/genome-repeats-detection.git>.

Conflict of interest statement. None declared.

References

- Al-Shayeb B, Sachdeva R, Chen L-X, Ward F, Munk P, Devoto A, Castelle CJ, Olm MR, Bouma-Gregson K, Amano Y, *et al.* Clades of huge phages from across Earth's ecosystems. *Nature* 2020;**578**(7795): 425–431. <https://doi.org/10.1038/s41586-020-2007-4>.
- Alempic J-M, Lartigue A, Goncharov AE, Grosse G, Strauss J, Tikhonov AN, Fedorov AN, Poirot O, Legendre M, Santini S, *et al.* An update on eukaryotic viruses revived from ancient permafrost. *Viruses* 2023;**15**(2):564. <https://doi.org/10.3390/v15020564>.
- Alonge M, Soyk S, Ramakrishnan S, Wang X, Goodwin S, Sedlazeck FJ, Lippman ZB, Schatz MC. RaGOO: fast and accurate reference-guided scaffolding of draft genomes. *Genome Biol.* 2019;**20**(1): 224. <https://doi.org/10.1186/s13059-019-1829-6>.
- Altschul SF, Gish W, Miller W, Myers EW, Lipman DJ. Basic local alignment search tool. *J Mol Biol.* 1990;**215**(3):403–410. [https://doi.org/10.1016/S0022-2836\(05\)80360-2](https://doi.org/10.1016/S0022-2836(05)80360-2).
- Andreani J, Aherfi S, Bou Khalil JY, Di Pinto F, Bitam I, Raoult D, Colson P, La Scola B. Cedratvirus, a double-cork structured giant virus, is a distant relative of pithoviruses. *Viruses*. 2016;**8**(11):300. <https://doi.org/10.3390/v8110300>.
- Andreani J, Khalil JYB, Baptiste E, Hasni I, Michelle C, Raoult D, Levasseur A, La Scola B. Orpheovirus IHUMI-LCC2: a new virus among the giant viruses. *Front Microbiol.* 2018;**8**:2643. <https://doi.org/10.3389/fmicb.2017.02643>.
- Aylward FO, Moniruzzaman M, Ha AD, Koonin EV. A phylogenomic framework for charting the diversity and evolution of giant viruses. *PLoS Biol.* 2021;**19**(10):e3001430. <https://doi.org/10.1371/journal.pbio.3001430>.
- Bäckström D, Yutin N, Jørgensen SL, Dharamshi J, Homa F, Zaremba-Niedwiedzka K, Spang A, Wolf YI, Koonin EV, Ettema TJG. Virus genomes from deep sea sediments expand the ocean megavirome and support independent origins of viral gigantism. *mBio* 2019;**10**(2):e02497–e02418. <https://doi.org/10.1128/mBio.02497-18>.
- Bertelli C, Mueller L, Thomas V, Pillonel T, Jacquier N, Greub G. *Cedratvirus lausannensis*—digging into Pithoviridae diversity. *Environ Microbiol.* 2017;**19**(10):4022–4034. <https://doi.org/10.1111/1462-2920.13813>.
- Besemer J, Lomsadze A, Borodovsky M. GeneMarkS: a self-training method for prediction of gene starts in microbial genomes. Implications for finding sequence motifs in regulatory regions. *Nucleic Acids Res.* 2001;**29**(12):2607–2618. <https://doi.org/10.1093/nar/29.12.2607>.
- Bisio H, Legendre M, Giry C, Philippe N, Alempic J-M, Jeudy S, Abergel C. Evolution of giant pandoravirus revealed by CRISPR/Cas9. *Nat Commun.* 2023;**14**(1):428. <https://doi.org/10.1038/s41467-023-36145-4>.
- Blanca L, Christo-Foroux E, Rigou S, Legendre M. Comparative analysis of the circular and highly asymmetrical marseilleviridae genomes. *Viruses* 2020;**12**(11):1270. <https://doi.org/10.3390/v12111270>.
- Boetzer M, Pirovano W. SSPACE-LongRead: scaffolding bacterial draft genomes using long read sequence information. *BMC Bioinformatics.* 2014;**15**(1):211. <https://doi.org/10.1186/1471-2105-15-211>.
- Bowater RP, Bohálová N, Brázda V. Interaction of proteins with inverted repeats and cruciform structures in nucleic acids. *Int J Mol Sci.* 2022;**23**(11):6171. <https://doi.org/10.3390/ijms23116171>.
- Boyer M, Yutin N, Pagnier I, Barrassi L, Fournous G, Espinosa L, Robert C, Azza S, Sun S, Rossmann MG, *et al.* Giant *Marseillevirus* highlights the role of amoebae as a melting pot in emergence of chimeric microorganisms. *Proc Natl Acad Sci U S A.* 2009;**106**(51):21848–21853. <https://doi.org/10.1073/pnas.0911354106>.
- Buchfink B, Xie C, Huson DH. Fast and sensitive protein alignment using DIAMOND. *Nat Methods.* 2015;**12**(1):59–60. <https://doi.org/10.1038/nmeth.3176>.
- Christo-Foroux E, Alempic J-M, Lartigue A, Santini S, Labadie K, Legendre M, Abergel C, Claverie J-M. Characterization of *Mollivirus kamchatka*, the first modern representative of the proposed molliviridae family of giant viruses. *J Virol.* 2020;**94**(8): e01997–e01919. <https://doi.org/10.1128/JVI.01997-19>.
- Cock PJ, Antao T, Chang JT, Chapman BA, Cox CJ, Dalke A, Friedberg I, Hamelryck T, Kauff F, Wilczynski B, *et al.* Biopython: freely available Python tools for computational molecular biology and bioinformatics. *Bioinformatics.* 2009;**25**(11):1422–1423. <https://doi.org/10.1093/bioinformatics/btp163>.
- Connelly JC, Kirkham LA, Leach DR. The SbcCD nuclease of *Escherichia coli* is a structural maintenance of chromosomes (SMC) family protein that cleaves hairpin DNA. *Proc Natl Acad Sci U S A.* 1998;**95**(14):7969–7974. <https://doi.org/10.1073/pnas.95.14.7969>.
- Crescente JM, Zavallo D, Helguera M, Vanzetti LS. MITE Tracker: an accurate approach to identify miniature inverted-repeat transposable elements in large genomes. *BMC Bioinformatics.* 2018;**19**(1):348. <https://doi.org/10.1186/s12859-018-2376-y>.
- Culyba MJ, Hwang Y, Minkah N, Bushman FD. DNA binding and cleavage by the fowlpox virus resolvase. *J Biol Chem.* 2009;**284**(2): 1190–1201. <https://doi.org/10.1074/jbc.M807864200>.
- Emms DM, Kelly S. OrthoFinder: phylogenetic orthology inference for comparative genomics. *Genome Biol.* 2019;**20**(1):238. <https://doi.org/10.1186/s13059-019-1832-y>.
- Filée J, Chandler M. Convergent mechanisms of genome evolution of large and giant DNA viruses. *Res Microbiol.* 2008;**159**(5):325–331. <https://doi.org/10.1016/j.resmic.2008.04.012>.
- Froelich-Ammon SJ, Gale KC, Osheroff N. Site-specific cleavage of a DNA hairpin by topoisomerase II. DNA secondary structure as a determinant of enzyme recognition/cleavage. *J Biol Chem.* 1994;**269**(10):7719–7725. [https://doi.org/10.1016/S0021-9258\(17\)37346-5](https://doi.org/10.1016/S0021-9258(17)37346-5).
- Garrido-Ramos MA. Satellite DNA: an evolving topic. *Genes (Basel).* 2017;**8**(9):230. <https://doi.org/10.3390/genes8090230>.
- Ge R, Mai G, Zhang R, Wu X, Wu Q, Zhou F. MUSTv2: an improved de novo detection program for recently active miniature inverted repeat transposable elements (MITEs). *J Integr Bioinforma.* 2017;**14**(3):20170029. <https://doi.org/10.1515/jib-2017-0029>.
- Hikida H, Okazaki Y, Zhang R, Nguyen TT, Ogata H. A rapid genome-wide analysis of isolated giant viruses using MinION sequencing. *Environ Microbiol.* 2023;**25**:2621–2635. <https://doi.org/10.1111/1462-2920.16476>.
- Jeudy S, Rigou S, Alempic J-M, Claverie J-M, Abergel C, Legendre M. The DNA methylation landscape of giant viruses. *Nat Commun.* 2020;**11**(1):2657. <https://doi.org/10.1038/s41467-020-16414-2>.
- Jiang N, Wessler SR. Insertion preference of maize and rice miniature inverted repeat transposable elements as revealed by the analysis

- of nested elements. *Plant Cell*. 2001;**13**(11):2553–2564. <https://doi.org/10.1105/tpc.010235>.
- Jones P, Binns D, Chang H-Y, Fraser M, Li W, McAnulla C, McWilliam H, Maslen J, Mitchell A, Nuka G, et al. InterProScan 5: genome-scale protein function classification. *Bioinformatics*. 2014;**30**(9):1236–1240. <https://doi.org/10.1093/bioinformatics/btu031>.
- Jumper J, Evans R, Pritzel A, Green T, Figurnov M, Ronneberger O, Tunyasuvunakool K, Bates R, Židek A, Potapenko A, et al. Highly accurate protein structure prediction with AlphaFold. *Nature*. 2021;**596**(7873):583–589. <https://doi.org/10.1038/s41586-021-03819-2>.
- Käll L, Krogh A, Sonnhammer EL. A combined transmembrane topology and signal peptide prediction method. *J Mol Biol*. 2004;**338**(5):1027–1036. <https://doi.org/10.1016/j.jmb.2004.03.016>.
- Katoh K, Standley DM. MAFFT multiple sequence alignment software version 7: improvements in performance and usability. *Mol Biol Evol*. 2013;**30**(4):772–780. <https://doi.org/10.1093/molbev/mst010>.
- Koonin EV, Dolja VV, Krupovic M, Varsani A, Wolf YI, Yutin N, Zerbini FM, Kuhn JH. Global organization and proposed megataxonomy of the virus world. *Microbiol Mol Biol Rev*. 2020;**84**(2):e00061–e00019. <https://doi.org/10.1128/MMBR.00061-19>.
- Lefkowitz EJ, Dempsey DM, Hendrickson RC, Orton RJ, Siddell SG, Smith DB. Virus taxonomy: the database of the International Committee on Taxonomy of Viruses (ICTV). *Nucleic Acids Res*. 2018;**46**(D1):D708–D717. <https://doi.org/10.1093/nar/gkx932>.
- Legendre M, Bartoli J, Shmakova L, Jeudy S, Labadie K, Adrait A, Lescot M, Poirot O, Bertaux L, Bruley C, et al. Thirty-thousand-year-old distant relative of giant icosahedral DNA viruses with a pandoravirus morphology. *Proc Natl Acad Sci U S A*. 2014;**111**(11):4274–4279. <https://doi.org/10.1073/pnas.1320670111>.
- Legendre M, Fabre E, Poirot O, Jeudy S, Lartigue A, Alempic J-M, Beucher L, Philippe N, Bertaux L, Christo-Foroux E, et al. Diversity and evolution of the emerging Pandoraviridae family. *Nat Commun*. 2018;**9**(1):2285. <https://doi.org/10.1038/s41467-018-04698-4>.
- Levasseur A, Andreani J, Dellerie J, Bou Khalil J, Robert C, La Scola B, Raoult D. Comparison of a modern and fossil pithovirus reveals its genetic conservation and evolution. *Genome Biol Evol*. 2016;**8**(8):2333–2339. <https://doi.org/10.1093/gbe/evw153>.
- Li N, Shi K, Rao T, Banerjee S, Aihara H. Structural insights into the promiscuous DNA binding and broad substrate selectivity of fowlpox virus resolvase. *Sci Rep*. 2020;**10**(1):393. <https://doi.org/10.1038/s41598-019-56825-w>.
- Liu Y, Bisio H, Toner CM, Jeudy S, Philippe N, Zhou K, Bowerman S, White A, Edwards G, Abergel C, et al. Virus-encoded histone doublets are essential and form nucleosome-like structures. *Cell*. 2021;**184**(16):4237–4250.e19. <https://doi.org/10.1016/j.cell.2021.06.032>.
- Lu S, Wang J, Chitsaz F, Derbyshire MK, Geer RC, Gonzales NR, Gwadz M, Hurwitz DI, Marchler GH, Song JS, et al. CDD/SPARCLE: the conserved domain database in 2020. *Nucleic Acids Res*. 2020;**48**(D1):D265–D268. <https://doi.org/10.1093/nar/gkz991>.
- Meštrović N, Mravinac B, Pavlek M, Vojvoda-Zeljko T, Šatović E, Plohl M. Structural and functional liaisons between transposable elements and satellite DNAs. *Chromosome Res*. 2015;**23**(3):583–596. <https://doi.org/10.1007/s10577-015-9483-7>.
- Mirdita M, Schütze K, Moriawaki Y, Heo L, Ovchinnikov S, Steinegger M. ColabFold: making protein folding accessible to all. *Nat Methods*. 2022;**19**(6):679–682. <https://doi.org/10.1038/s41592-022-01488-1>.
- Mönttinen HAM, Bicep C, Williams TA, Hirt RP. The genomes of nucleocytoplasmic large DNA viruses: viral evolution writ large. *Microb Genom*. 2021;**7**(9):000649. <https://doi.org/10.1099/mgen.0.000649>.
- Moreira D, Brochier-Armanet C. Giant viruses, giant chimeras: the multiple evolutionary histories of Mimivirus genes. *BMC Evol Biol*. 2008;**8**(1):12. <https://doi.org/10.1186/1471-2148-8-12>.
- Nguyen L-T, Schmidt HA, von Haeseler A, Minh BQ. IQ-TREE: a fast and effective stochastic algorithm for estimating maximum-likelihood phylogenies. *Mol Biol Evol*. 2015;**32**(1):268–274. <https://doi.org/10.1093/molbev/msu300>.
- Notredame C, Higgins DG, Heringa J. T-Coffee: a novel method for fast and accurate multiple sequence alignment. *J Mol Biol*. 2000;**302**(1):205–217. <https://doi.org/10.1006/jmbi.2000.4042>.
- O’Leary NA, Wright MW, Brister JR, Ciufu S, Haddad D, McVeigh R, Rajput B, Robbertse B, Smith-White B, Ako-Adjei D, et al. Reference sequence (RefSeq) database at NCBI: current status, taxonomic expansion, and functional annotation. *Nucleic Acids Res*. 2016;**44**(D1):D733–D745. <https://doi.org/10.1093/nar/gkv1189>.
- Prijbelski A, Antipov D, Meleshko D, Lapidus A, Korobeynikov A. Using SPAdes de novo assembler. *Curr Protoc Bioinformatics*. 2020;**70**(1):e102. <https://doi.org/10.1002/cpbi.102>.
- Queiroz VF, Carvalho JVRP, de Souza FG, Lima MT, Santos JD, Rocha KLS, de Oliveira DB, Araújo JP Jr, Ullmann LS, Rodrigues RAL, et al. Analysis of the genomic features and evolutionary history of pithovirus-like isolates reveals two major divergent groups of viruses. *J Virol*. 2023;**97**(7):e0041123. <https://doi.org/10.1128/jvi.00411-23>.
- R Core Team. R: a language and environment for statistical computing. Vienna, Austria. 2021. Available from: <https://www.R-project.org/>
- Rice P, Longden I, Bleasby A. EMBOS: the European Molecular Biology Open Software Suite. *Trends Genet*. 2000;**16**(6):276–277. [https://doi.org/10.1016/S0168-9525\(00\)02024-2](https://doi.org/10.1016/S0168-9525(00)02024-2).
- Rigou S, Santini S, Abergel C, Claverie J-M, Legendre M. Past and present giant viruses diversity explored through permafrost metagenomics. *Nat Commun*. 2022;**13**(1):5853. <https://doi.org/10.1038/s41467-022-33633-x>.
- Rodrigues RAL, Andreani J, Andrade ACDSP, Machado TB, Abdi S, Levasseur A, Abrahão JS, La Scola B. Morphologic and genomic analyses of new isolates reveal a second lineage of cedratviruses. *J Virol*. 2018;**92**(13):e00372–e00318. <https://doi.org/10.1128/JVI.00372-18>.
- Rodríguez-R LM, Konstantinidis KT. The enveomics collection: a toolbox for specialized analyses of microbial genomes and metagenomes. 2016. Available from: <https://peerj.com/preprints/1900>
- Schulz F, Alteio L, Goudeau D, Ryan EM, Yu FB, Malmstrom RR, Blanchard J, Woyke T. Hidden diversity of soil giant viruses. *Nat Commun*. 2018;**9**(1):4881. <https://doi.org/10.1038/s41467-018-07335-2>.
- Senkevich TG, Yutin N, Wolf YI, Koonin EV, Moss B. Ancient gene capture and recent gene loss shape the evolution of orthopoxvirus-host interaction genes. *mBio*. 2021;**12**(4):e0149521. <https://doi.org/10.1128/mBio.01495-21>.
- Silva LKDS, Andrade ACDSP, Dornas FP, Rodrigues RAL, Arantes T, Kroon EG, Bonjardim CA, Abrahão JS. Cedratvirus getuliensis replication cycle: an in-depth morphological analysis. *Sci Rep*. 2018;**8**(1):4000. <https://doi.org/10.1038/s41598-018-22398-3>.
- Snipen L, Liland KH. micropan: an R-package for microbial pan-genomics. *BMC Bioinformatics*. 2015;**16**(1):79. <https://doi.org/10.1186/s12859-015-0517-0>.
- Steinegger M, Söding J. MMseqs2 enables sensitive protein sequence searching for the analysis of massive data sets. *Nat Biotechnol*. 2017;**35**(11):1026–1028. <https://doi.org/10.1038/nbt.3988>.
- Sun C, Feschotte C, Wu Z, Mueller RL. DNA transposons have colonized the genome of the giant virus Pandoravirus salinus. *BMC Biol*. 2015;**13**(1):38. <https://doi.org/10.1186/s12915-015-0145-1>.
- Tarchini R, Biddle P, Wineland R, Tingey S, Rafalski A. The complete sequence of 340 kb of DNA around the rice Adh1-adh2 region reveals interrupted colinearity with maize chromosome 4.

- Plant Cell*. 2000;**12**(3):381–391. <https://doi.org/10.1105/tpc.12.3.381>.
- Tettelin H, Massignani V, Cieslewicz MJ, Donati C, Medini D, Ward NL, Angiuoli SV, Crabtree J, Jones AL, Durkin AS, *et al*. Genome analysis of multiple pathogenic isolates of *Streptococcus agalactiae*: implications for the microbial “pan-genome”. *Proc Natl Acad Sci U S A*. 2005;**102**(39):13950–13955. <https://doi.org/10.1073/pnas.0506758102>.
- Thakur J, Packiaraj J, Henikoff S. Sequence, chromatin and evolution of satellite DNA. *Int J Mol Sci*. 2021;**22**(9):4309. <https://doi.org/10.3390/ijms22094309>.
- Thomas V, Bertelli C, Collyn F, Casson N, Telenti A, Goesmann A, Croxatto A, Greub G. Lausannevirus, a giant amoebal virus encoding histone doublets. *Environ Microbiol*. 2011;**13**(6):1454–1466. <https://doi.org/10.1111/j.1462-2920.2011.02446.x>.
- Tria FDK, Landan G, Dagan T. Phylogenetic rooting using minimal ancestor deviation. *Nat Ecol Evol*. 2017;**1**(7):1–7. <https://doi.org/10.1038/s41559-017-0193>.
- van Kempen M, Kim SS, Tumescheit C, Mirdita M, Lee J, Gilchrist CLM, Söding J, Steinegger M. Fast and accurate protein structure search with Foldseek. *Nat Biotechnol*. 2023. <https://doi.org/10.1038/s41587-023-01773-0>.
- Wick RR, Judd LM, Gorrie CL, Holt KE. Unicycler: resolving bacterial genome assemblies from short and long sequencing reads. *PLoS Comput Biol*. 2017;**13**(6):e1005595. <https://doi.org/10.1371/journal.pcbi.1005595>.
- Yang Z. PAML: a program package for phylogenetic analysis by maximum likelihood. *Comput Appl Biosci*. 1997;**13**(5):555–556. <https://doi.org/10.1093/bioinformatics/13.5.555>.
- Yuan Y, Gao M. Jumbo bacteriophages: an overview. *Front Microbiol*. 2017;**8**:403. <https://doi.org/10.3389/fmicb.2017.00403>.
- Zhang XY, Feschotte C, Zhang Q, Jiang N, Eggleston WB, Wessler SR. P instability factor: an active maize transposon system associated with the amplification of Tourist-like MITEs and a new superfamily of transposases. *Proc Natl Acad Sci U S A*. 2001;**98**(22):12572–12577. <https://doi.org/10.1073/pnas.211442198>.
- Zhang H-H, Zhou Q-Z, Wang P-L, Xiong X-M, Luchetti A, Raoult D, Levasseur A, Santini S, Abergel C, Legendre M, *et al*. Unexpected invasion of miniature inverted-repeat transposable elements in viral genomes. *Mob DNA*. 2018;**9**(1):19. <https://doi.org/10.1186/s13100-018-0125-4>.
- Zhou Z-H, Akgün E, Jasim M. Repeat expansion by homologous recombination in the mouse germ line at palindromic sequences. *Proc Natl Acad Sci U S A*. 2001;**98**(15):8326–8333. <https://doi.org/10.1073/pnas.151008498>.
- Zuker M. mFold web server for nucleic acid folding and hybridization prediction. *Nucleic Acids Res*. 2003;**31**(13):3406–3415. <https://doi.org/10.1093/nar/gkg595>.